UNIVERSITY OF OKLAHOMA

GRADUATE COLLEGE

USE OF LOW-RESOLUTION BURNED AREA PRODUCTS AND IMPLICATIONS FOR FIRE RISK ASSESSMENT WITHIN THE WILDLAND-URBAN INTERFACE

A THESIS

SUBMITTED TO THE GRADUATE FACULTY

in partial fulfillment of the requirements for the

Degree of

MASTER OF SCIENCE IN GEOGRAPHY

By

Haley Smith

Norman, Oklahoma

2019

USE OF LOW-RESOLUTION BURNED AREA PRODUCTS AND IMPLICATIONS FOR FIRE RISK ASSESSMENT WITHIN THE WILDLAND-URBAN INTERFACE

A THESIS APPROVED FOR THE DEPARTMENT OF GEOGRAPHY AND ENVIRONMENTAL SUSTAINABILITY

BY

Dr. Kirsten de Beurs, Chair

Dr. Thomas Neeson

Dr. Jeffrey Widener

Acknowledgments

Financial support for this thesis was provided through the Oklahoma Space Grant and the NSF NRT Program. I would like to thank my family, friends and professors for all of the encouragement and support they provided me while working to complete this thesis. Specifically, I would like to thank my mother for all of the long nights that she stayed up listening to me and encouraging me. Words cannot describe how wonderful I think you are or how lucky I am to have someone as gracious and loving as you for a mom. I would also like to thank my sister, Lindsay, for all of her encouragement and advice that helped me along the way. Additionally, I would like to give tremendous thanks to my advisor, Dr. Kirsten de Beurs and committee members Dr. Thomas Neeson and Dr. Jeffrey Widener for believing in my ability to finish my thesis and providing me with the counsel to do so despite a rocky start – I would not have finished without your help and insight. I would also like to thank Dr. Jonathan Kujawa for his endless encouragement and support and advice. Thank you for fostering my desire to learn and create knowledge since I was an undergraduate student; you taught me that I also have the ability to add something valuable to academia. Finally, I would like to thank Stephanie Garrison and her team for all of their support over the years. Thank you for your incessant willingness to genuinely listen to me and to help me find new solutions whenever I needed them.

TABLE OF CONTENTS

List of Tables

List of Figures

Use of low-resolution burned area products and implications for fire risk assessment within the wildland-urban interface

Abstract:

The impacts of wildfires are socially, economically and ecologically vast and these impacts are often thought to be intensified within the wildland-urban interface (WUI) where structures intermingle with wildland vegetation. Because the WUI is expanding rapidly and ignitions within the WUI are said to occur more frequently, it is pertinent that fire scientists and land managers have access to accurate fire occurrence and burned area data within these regions. Burned area information is often accessed via remotely sensed burned area products of differing spatial resolutions. It is known that burned area products with coarse spatial resolution frequently underestimate burned area due to the omission of small fires; therefore, this thesis aims to explore how much burned area low-resolution BA products miss, where they miss burned area, and how different products detect burned area within the wildland-urban interface in Oklahoma, USA. In order to determine how much burned area is missed by these products and where the burned area is located in regards to the WUI, this project utilizes the MODIS MCD64A1 burned area product and the Monitoring Trends in Burn Severity (MTBS) data as a proxy for coarse-resolution burned area data and compares it to a higher-resolution dataset developed using Sentinel-2 imagery. We find that the low-resolution products are unable to detect a significant amount of burned area (Δ 57,000 acres) and may poorly depict the spatial distribution of fire as they were unable to detect major hotspots of fire occurrence. Additionally, we find that the majority of burned area within our study region (Eastern Oklahoma, USA) takes place outside of the WUI.

Keywords: burned Area, wildland-urban interface, remote sensing, spatial resolution

1. Background

Remote Sensing is the science of acquiring and analyzing information about objects or phenomena from a distance. The sun radiates electromagnetic (EM) energy. This energy, when differentiated by wavelength and frequency, is categorized by the electromagnetic spectrum (EMS). When EM energy from the sun hits the surface of the earth, the light interacts with a variety of molecules and surfaces. While some of this light is scattered within our atmosphere and back into space, a portion of it makes it to the surface of the earth where it interacts with matter on the Earth's surface (trees, bodies of water, buildings, etc.) Different types of matter reflect, absorb and emit EM energy differently within different portions of the EMS, thereby giving every object (with a unique chemical composition) a unique spectral profile (Kennedy et. al., 2009). When optical energy from the sun is reflected back off of the surface of the earth, optical remote sensing satellites are used to detect this reflected electromagnetic energy. Therefore, the capacity to store the spectral information for a given region at a given time makes remote sensing an invaluable tool when studying change detection. The basis of using remote sensing for change detection is that changes in the object or phenomena of interest will induce spectral changes in said object/phenomena thereby allowing us to identify changes in the object over time (Hussain et. al., 2013.).

Because remotely-sensed imagery can capture phenomena from local to regional to even global scales, it is an invaluable tool for studying and detecting changes in phenomena that occur at a variety of spatial and temporal scales such as wildfires (Lentile et. al., 2006). Remote sensing can detect regions affected by fires because burned vegetation gives off a radically different spectral signal than unburned vegetation due to the dark carbon residue (char) that is created when the vegetation is exposed to flame (Trigg and Flasse, 2000; Pereira, 2003).

Additionally, in regions where char is quickly disseminated by wind, sensors are still often able to detect the removal of photosynthetic vegetation (Koutsias et. al., 2000).

The impacts of wildfires are expansive and increasing global temperatures and decreasing precipitation rates will most likely lead to upturns in the number of wildfires and forest fires experienced *and* the total area burned during these events (Flannigan et. al., 2009; Gitas et. al, 2012). Because of this, wildfire managers and fire scientists require quality fire occurrence information in order to mitigate future fire risks (Oliveira et. al., 2012). As a response to this need, a variety of remotely-sensed burned area data products were developed. However, many of these products that are still used today, such as the MODIS MCD64A1 burned area product or the PROBA-V product which have relatively coarse spatial resolutions, or fields-of-view (500 meters and 300 meters, respectively.) Coarse spatial resolution, as it applies to the detection of burned area, can be of issue as larger fields-of-view are often unable to detect small fires. Hence, it is possible that the use of these large-scale burned area products could lead to underestimations in total burned area due to the omission of small fires (Hall et. al., 2016; Nogueira et. al., 2017; Zhu et. al., 2017) which is alarming as burned area information is often utilized to assess economic losses, ecological impacts, monitor land-cover changes, and model the atmospheric impacts of burning (Gitas et. al., 2004; Pereira, 2003).

Hence, this work aims to compare two commonly-used, coarse-resolution burned area products (the MODIS MCD64A1 burned area, and Monitoring Trends in Burn Severity product) to a higher-resolution, Sentinel-2 (20-meter spatial resolution) burned area dataset. In doing so, we aim to explore just how much burned area these low-resolution products miss, where they miss burned area, and how the different products detect burned area within the wildland-urban interface.

2. Wildfire and the wildland-urban interface

Impacts from wildfires are vast and complex with the potential of fires to change vegetation dynamics (Padilla et. al., 2015), degrade air quality (Fann et. al., 2018), and increase greenhouse gas emissions (Stavros et. al., 2014). Additionally, increasing global temperatures and decreasing precipitation will most likely lead to upturns in the number of wildfires and forest fires experienced *and* the total area burned during these events (Flannigan et. al., 2009; Gitas et. al, 2012) therefore indicating a positive feedback loop between fire and climate (Stavros et. al., 2014). This becomes cause for concern when considering the implications of fire interaction within the wildland-urban interface (WUI), or "the area in which houses meet or intermingle with undeveloped wildland vegetation" (Radeloff et al., 2005) as fire ignitions have been found to occur nearly twice as frequently in wildland-urban interface regions (Chas-Amil et al., 2013). As the WUI continues to expand and as rising numbers of people begin to settle within these previously uninhabited regions (Theobald & Romme, 2007), increased fragmentation of these wildland ecosystems and their consequent intermingling with urban structures is cause for concern. Especially, since previous literature has shown that landscape heterogeneity and structure have large implications in regard to fire behavior. For example, Herrero-Corral et. al. (2012) found a correlation between fuel homogeneity and fire risk, noting that certain spatial configurations of buildings within the WUI influenced landscape structure increase fire risk. Similarly, Ortega et. al. (2012) found that the areas most vulnerable to wildfires in Spain experienced increased landscape fragmentation, noting that fine-grained forest-agriculture mixtures had "an ignition frequency four times higher than that of pure forested landscapes" (Ortega et. al., 2012; Herrero-Corral et. al., 2012).

Fire occurrence information (here, referring to the spatial distribution and intensity of

fires) aids in the determination of fire risk by indicating where ignition sources are located and where there are favorable conditions for fire spread (Oliveira et. al., 2012). Therefore, in order to properly plan for and mitigate fire risk within the WUI, fire management teams and policy makers often depend on information regarding both fire occurrence and the spatial patterns of human settlement across the area of concern (Moreno et. al, 2011; Chas- Amil et. al., 2013).

Burned vegetation gives off a radically different spectral signal than unburned vegetation due to the dark carbon residue (char) that is created when the vegetation is exposed to flame. As a result, remotely sensed imagery is capable of observing burned areas on the ground. As our climate warms, the imminent need for accurate burned area and fire occurrence data has led to the development of a variety of remotely sensed global burned area products over the years. Earlier burned area products which are no longer available include the Global Burnt Surfaces (GBS) product derived from weekly composites of the daily NOAA-AVHRR GAC 8 km dataset providing data ranging from 1982-1999 (Carmona-Moreno et. al., 2005); the GLOBCARBON product derived from SPOT Vegetation, ASTR-2, MERIS and AATSR data (available in 10km, 1 km, 0.5 degree and 0.25 degree spatial resolution) with data ranging from 1998-2007 (Plummer et. al., 2006); the Geoland-2 product derived from 1 km SPOT Vegetation data with a temporal range of 1999- 2014; the Global Burnt Area 2000 (GBA2000) product which utilized 1 km SPOT Vegetation data for the year 2000 (Grégoire et. al., 2003); the GLOBSCAR product which utilized 1 km ATSR-2 data for the year 2000 (Simon et. al., 2004) and the L3JRC product which utilized 1 km SPOT Vegetation data and had a temporal coverage of 2000-2007 (Tansey et. al., 2007). Currently available burned area products are described in Table 1. Of the currently available products, this work focuses on the MODIS Burned Area Product (MCD64A1) and the Monitoring Trends in Burn Severity (MTBS) burned area product as they are freely available

products with a large temporal coverage that have been used in recent fire research (see Radeloff et. al., 2018; Kramer et. al., 2018; Zhu et. al., 2017; etc.)

The aforementioned burned area products utilize a variety of vegetation indices in order to identify burned areas. For example, the FIRECCILT10 product utilizes the Burn Area Index (BAI) and the Global Environmental Monitoring Index (GEMI); the MTBS products utilize the Normalized Burn Ratio (NBR), the Differenced Normalized Burn Ratio (dNBR) and the Relativized Differenced Normalized Burn Ratio (RdNBR); while Products such as GFED4 and MODIS MCD64A1 utilize their own vegetation indices. For a more comprehensive list of vegetation indices commonly used in burned area detection and their formulas see Fornacca et. al., (2018) and Chu & Guo (2014). In this paper, we will use the Normalized Burn Ratio (NBR) as it has become known as the "standard spectral index to estimate fire/burn severity" (Veraverbeke et. al., 2010).

The wildland-urban interface/intermix has been defined as "the area in which houses meet or intermingle with undeveloped wildland vegetation" (Radeloff et al., 2005) and therefore encompasses homes or structures built within densely forested areas, shrublands and grasslands. Homes within the WUI comprise more than 39% of all houses in the contiguous United States with the WUI as a whole encompassing more than 9% of the total land area (Radeloff et al., 2005). The development of these structures amongst previously wild vegetation has led to the destruction of homes by wildfire, increased land/habitat fragmentation, the introduction of invasive species and an overall loss of biodiversity (Hansen et al., 2005; Liu, Wimberly, Lamsal, Sohl, & Hawbaker, 2015). Despite this, the WUI continues to develop rapidly, with a 52% increase in total occupied land mass occurring between 1970 and 2000 and projections into 2030 indicating an additional 10% increase (Theobald & Romme, 2007). As the wildland-urban

interface continues to expand, wildfire has become a topic of increasing concern with nearly 45% of the structures located within the WUI were at risk for burning (defined by having already experienced 1 fire) between the years 2000 and 2010 (Thomas & Butry, 2014).

The spatial resolution of a dataset can affect the reported burned area. For example, large-scale remotely sensed fire products such as the Monitoring Trends in Burn Severity (MTBS) products (which maps fires 500 acres or greater in the eastern US, and fires 1000 acres or larger in the Western US) or the Moderate Resolution Imaging Spectroradiometer (MODIS) MCD64A1 burned area product (with a spatial resolution of 500m or approximately 62 acres per pixel) are often relied upon by researchers in order to estimate burned area (see Dennison et. al., 2014; Libonati et. al., 2015; Sparks et. al., 2015, Radeloff et. al., 2018). Likewise, many studies surrounding wildfire and the WUI use gridded fire data of 30-meters or greater (Martinez et. al., 2009; Badia et. al., 2011; Radeloff et. al., 2018). It is possible that the scale of coarse pixel fire products could lead to underestimations in total burned area due to the omission of small fires (Hall et. al., 2016; Nogueira et. al., 2017; Zhu et. al., 2017) therefore introducing significant error.

Radeloff et. al (2018) found that rapid growth of the WUI has led to increased wildfire risk, using the number of housing units within burned areas as a proxy for fire risk. They found a 62% growth in the number of housing units located within a fire's perimeter between 1990 and 2010 in the US indicating substantial occupation within high-risk fire areas. However, since MTBS dataset was used to quantify burned area, it is possible that the number of housing units within burned areas was underestimated. Although there are discrepancies between the total burned area reported by various global BA products, smaller-scale assessments using high resolution imagery indicate high underestimations in burned area (Nogueira et. al., 2016) and

some estimate that if small fires were properly accounted for, the global total burned area would increase by approximately 35% (Randerson, et. al., 2012).

Radeloff et al. (2018) provide a compelling analysis of the increased fire risk within the WUI; however, they focus on fires that are 500 acres and larger. Here we are interested in understanding whether the number and area of small fires (< 500 acres) follows the same spatial pattern. This project uses Sentinel-2 MSI data and the differenced Normalized Burn Ratio (dNBR) as a proxy for small fire occurrence within the WUI to better understand what remotely sensed burned area products such as the MTBS and MODIS MCD64A1 burned area products are missing. In addition, we evaluate data from the national fire incident reporting system to further identify the number of small fires occurring in our study area of eastern Oklahoma, USA. Fire-related research in Oklahoma has been mainly focused on the response of different species to fire (Boyd & Bidwell, 2001; Allred et. al., 2011; Bright et. al., 2016), fire history throughout the state (Clark et. al., 2007; Allen & Palmer, 2011; Stambaugh et. al., 2013), fire danger estimation (Carlson et al, 2002; Carlson and Burgan, 2003.), and specific environmental factors influencing wildfires such as weather (Reid et al., 2010) or soil moisture (Krueger et al., 2015). Some research has focused on the Flint Hills corridor stretching from northern Oklahoma to eastern Kansas where prescribed burning is commonplace (Mohler & Goodin, 2012). However, few, if any, researchers to date that have calculated burned area and fire occurrence using higher-resolution remotely-sensed imagery (Mohler & Goodin utilized MODIS data) in Oklahoma.

2.1 Study Area

Our study area is approximately 23,080 km^2 of land located within eastern Oklahoma, USA (Figure 1). The study area is comprised predominantly of forest (45%), grassland (17%) and

croplands (25%) (Yang et. al., 2018). As of 2010, the wildland-urban intermix in Oklahoma comprised a total of 10,486 km^2 while the wildland-urban interface comprised 3,198 km^2. Cumulatively this represents a total WUI area of 13,684 km^2, approximately 7.6 percent of the states total land area. This figure is slightly higher for our study area, which, as of 2010, consisted of approximately 7.23% or 1,669 km^2 wildland-urban intermix, and approximately 2.87% or 662 km^2 wildland-urban interface with the intermix growing most rapidly; having increased by 2.17% since 1990 (the interface only saw increases of about .79% between 1990 and 2010). The main cities within our study area include Broken Arrow (2010 population of 98,850), Sapulpa (2010 population of 20,544), Muskogee (2010 population of 39,223) and McAlester (2010 population of 18,363); however, the region also encompasses the southern portion of the Tulsa metropolitan area. Tulsa, with a population of 391,906 according to the 2010 census, is the second largest city in the state of Oklahoma (U.S. Census Bureau, 2010.).

2.2 Data

2.2.1 Burned area data

In this project we first generate a high resolution (20m) burned area dataset based on Sentinel-2A data, which is then compared to Landsat based MTBS data (30m) and the MODIS MCD64A1 burned area product (500m) which are two freely available burned area datasets that are often used in burned area analysis. Point data from the National Fire Incident Reporting System is also evaluated.

2.2.2 Sentinel-2 data

Relatively cloud-free level 1C orthorectified Sentinel-2A MSI Imagery was downloaded through the European Space Agency Copernicus Open Access Hub in the Sentinel Standard Archive Format for Europe (SAFE format). The level 1C product comes as Top-Of-Atmosphere reflectances in 100x100 kilometer tiles with a UTM/WGS84 projection. Note that our imagery was from UTM zone 15. The temporal resolution of Sentinel 2A is approximately 10 days while the spatial resolution of the sensor is reliant on the spectral band. We used the 20-meter spatial resolution which is associated with a spectral resolution consisting of five bands: B5 (705 nm), B6 (740 nm), B7 (783 nm), B8a (865 nm), B11 (1610 nm) and B12 (2190 nm). Our study area was comprised of two Sentinel-2A MSI tiles with tile T15STV representing the northern half of the study area and tile T15STU representing the southern half. We downloaded prefire (December / January) and postfire (March) imagery for both tiles (Table 2). We atmospherically corrected the level 1C products and converted them into level 2A products of 20-meter resolution using the Sen2Cor processor in ESA SNAP.

2.2.3 Monitoring Trends in Burn Severity (MTBS) data

National fire occurrence point data and burn severity rasters were obtained through the Monitoring Trends in Burn Severity (MTBS) program. MTBS data represents all large fires 1000 acres (~ 4 km^2) or greater for the Western United States and 500 acres (~2 km^2) or greater for the Eastern portion of the United States with Oklahoma being classified as a western state. MTBS data is developed based on Landsat Thematic Mapper (TM) and Enhanced Thematic Mapper Plus (ETM+) satellite data and therefore has a spatial resolution of 30 meters and contains data going back until 1984 (as Landsat TM was not launched until 1982). MTBS products are created by first obtaining fire occurrence data from the Integrated Reporting of Wildland-Fire Information (IRWIN) project and compiling the data into an MTBS database. For fires over 1000 acres, Landsat reflectance imagery of the reported fire location and ignition date (both before and after the fire) are obtained and undergo geometric and radiometric correction. Then, using Landsat TM bands 4 (near infrared) and 7 (short-wave infrared), the Normalized Burn Ratio (NBR= (TM4-TM7)/(TM4+TM7)) is computed for each pre-fire and post-fire image, followed by the differenced Normalized Burn Ratio (dNBR= $NBR_{prefire}$ - $NBR_{postfire}$) and Relativized dNBR (RdNBR= dNBR/$\sqrt{\left|\frac{NBR_{prefire}}{1000}\right|}$) in order to characterize fire severity. An MTBS mapping analyst then hand digitizes the fire perimeter based off of the reflectance imagery and the NBR, dNBR and RdNBR imagery and interprets the burn severity classes for the fire (Eidenshink et. al., 2007).

2.2.4 MODIS MCD64A1

The MODIS burned Area product, MODIS MCD64A1, is a monthly product derived from daily 500m surface reflectance inputs in conjunction with 1 km MODIS active fire observations. The

algorithm calculates the normalized burn ratio using composite reflectance imagery from MODIS bands 5 (near—infrared 2) and 7 (short-wave infrared 2) in which Burn Ratio = (b5 – b7/ b5 + b7) to create dynamic burn thresholds on a per-pixel basis. In the resulting product each pixel value indicates the day of the year that the pixel burned with a range of 1-366 while values of 0 indicate unburned pixels (Giglio et. al., 2016). MODIS uses a sinusoidal coordinate system comprised of tiles and for our study area we used tile (h10, v5). For this study we used data from the month of February in 2016.

2.2.5 National Fire Incident Reporting System point data

Fire occurrence data for 2016 was obtained directly through the National Fire Incident Reporting System (NFIRS) state program manager for the state of Oklahoma. This data contained complete street addresses for each fire location as reported by 273 unique fire departments across 68 counties in Oklahoma. Per the U.S. Fire administration, Oklahoma has a total of 745 registered fire departments (as of December 2018) indicating that the 6,013 reported fires within our records likely represent only of subset of all fires experienced within the region. In addition to fire location, the fires were marked with fire department ID and name, alarm date and time, incident type and description (i.e. grass fire, brush fire, etc.), monetary loss and total number of acres burned per fire. This data was utilized to determine the month with the greatest number of wildland fire occurrence in the state.

2.2.6 Ancillary datasets

2.2.6.1 National Land Cover Database

We obtained National Land Cover Database (NLCD) land cover classification data for the contiguous United States in 2011. NLCD data comes at a 30-meter spatial resolution and contains 16 land cover categories based off of a modified Anderson Level II classification scheme (Yang et. al., 2018). We use the 2011 land cover product that was amended in 2014 to correct for the over-elimination of small areas within the four classes categorized as "developed" or urban.

2.2.6.2 Wildland Urban Interface

The wildland urban *intermix* has been defined as a region containing more than 1 housing unit per every 40 acres of land that is also covered by more than 50% wildland vegetation. The wildland urban *interface*, is defined as having more than one housing unit per every 40 acres of land and containing less than 50% wildland vegetation while being within 1.5 miles of a large area (greater than 1,235 acres) that is covered with more than 75% wildland vegetation (Stewart et. al., 2007). In order to quantify the WUI and WUIx for our study area, we use 30-meter resolution data for the state of Oklahoma for 2010. This data was created by the SILVIS lab and generated using the NLCD 2011, NLCD 2001 and NLCD 1992/2001 Retrofit Change Product for land cover data and the U.S. Census TIGER 2010 block polygons with associated 2010, 2000, and 1990 housing and population density to quantify human presence (Radeloff et. al., 2017).

2.3 Methods

As mentioned before, there are several remotely sensed burned area datasets available, many of which have low spatial resolution. Because of this, we sought to develop our own dataset using 20-meter resolution Sentinel-2 data in order to better quantify small fire occurrence. We then aim to compare this higher-resolution Sentinel-based dataset to existing burned area products in order to understand how much burned area these low-resolution products are missing and where these underestimations are occurring. For example, what is the distribution of fire occurrence reported by each product? Are these products underestimating burned area within the WUI? In order to accomplish this, we compare our Sentinel-2 dataset with the MTBS and MODIS MCD64A1 Burned area products, which are both easily accessible, frequently-used, large-scale burned area products. Our comparison was divided into four main parts: 1) an initial comparison using a sample of the data; 2) a comparison of the burned area reported by each product for fires of different sizes; 3) a comparison of the spatial distributions of fire occurrence reported by each product; and 4) a quantification of fire occurrence and burned area within the WUI for each dataset.

2.3.1 Sentinel dataset development

We began by creating our own dataset utilizing the Sentinel-2A data. Using the same methods as the MTBS data, we calculated the Normalized Burn Ratio ($NBR = \frac{NIR-SWIR}{NIR+SWIR}$) for each pre-fire and post fire image using Sentinel band 8a for the near-infrared (NIR) and band 12 for the short-wave infrared (SWIR). The differenced Normalized Burn Ratio ($dNBR = NBR_{prefire} - NBR_{postfire}$) was then calculated using the NBR images for each respective tile and used the thresholds suggested by the USGS FireMon program (Lutes et. al., 2006) to determine fire severity. We

then used a freely available water mask to remove water from the imagery (Jean-Francois et. al., 2016). Last, we used band math to create binary rasters from our masked dNBR images in which 1 represented fire pixels (as categorized by threshold values indicating burned area) and zero represented all other features.

2.3.2 Fire Dataset Comparison

2.3.2.1 Comparison of MTBS sample

In order to determine whether or not our three primary fire data products (the Sentinel-2 based dNBR calculated by hand, the MODIS MCD64A1 burned area product and the MTBS product) were comparable, we identified all fires over 1000 acres in our study area in February 2016 (which is the month with the largest number of fires in our study area (Figure 2)) for each product and charted the BA reported by each product.

2.3.2.2 BA size comparison

Next, we compared the datasets for fires at a variety of different burned area size thresholds. MTBS data maps all fires over 1000 acres in the western United States, including Oklahoma (Eidenshink et. al., 2007). In order to determine the burned area that is unaccounted for due to the omission of small fires, different acreage thresholds of 10,000, 5000, 2000, 1000, 750, 500, 250, 100, 50, 20, and 10 acres (i.e. calculating the burned area for all fires over 10,000 acres, over 5000 acres, over 2000 acres, etc.) were calculated for each dataset. We then determined the number of fires and burned area for each fire for each threshold. Note that we did not apply thresholds below 50 acres for the MODIS product as the size of one MODIS pixel is approximately 60 acres and therefore would have been redundant. To filter out noise due to

water and cropland changes, these land covers were masked based on the European Commission's Joint Research Center Global Surface Water dataset (Pekel et al. 2016), and the USDA National Agricultural Statistics Service Cropland Data Layer, 2016, respectively.

2.3.2.3 Distribution comparison

We converted our burned area data for fires 500 acres and greater from raster format to vector point data. We then measured the first-order effects of each point pattern. First order effects, which quantitatively describe spatial variation in the intensity of a point pattern, were estimated via the kernel-smoothed intensity function, λ(x) (the estimated intensity of a pattern at some point x), as follows: $\lambda_t(x)=\frac{1}{p_t(x)}\sum_{i=1}^{n}\delta_t(x-x_i)$ In which $x_i=\{x_1,x_2,\cdots,x_n\}$ for the number of points $n\in\mathbb{R}$, where δ_t is the Gaussian smoothing kernel, $\frac{1}{p_t(x)}$ is an edge correction factor and $t>0$ determines the amount of smoothing (Diggle, 1985; Yang et al., 2007). By performing an intensity analysis on the point patterns created for each dataset, we characterize the spatial distribution of the fire locations and determine where fire events are more likely to occur across space.

2.3.2.4 Fire wildland-urban interface analysis

We calculated the burned area occurring within the wildland-urban interface, wildland-urban intermix, urban areas, and wildlands (here, defined as all other regions that could not be categorized into the three aforementioned categories.) WUI and WUI_x regions were classified using the 30-meter resolution data by Radeloff et al (2017) while urban areas and all other remaining areas were categorized using the NLCD 2011 land cover classification layer. Fire polygons for each dataset were then overlayed to determine how many pixels from each region

(Wildland, Urban, WUI, WUI_x) were within the fire boundaries and the percentage of the total burned area that each category took up within the fire perimeters for each dataset.

2.4 Results

False color composites of pre and post-fire images reveal that burned areas are easily visible in the Sentinel-2 datasets (Figure 3). The dNBR dataset is able identify and highlight the burned areas (Figure 3).

2.4.1 MTBS comparison results

In order to determine whether our three primary fire data products (the Sentinel-2 based dNBR calculated by hand, the MODIS MCD64A1 burned area product and the MTBS product) were able to identify the same fires, we compared the total acres burned for each dataset. MTBS reported 13 fires for the month of February 2016; however, upon further inspection, one of the fires appears to just be a sandbank and therefore we only analyze the 12 remaining fires. Our results for the remaining 12 fires indicate that each dataset produced similar burned area values with a greater difference in burned area seen for larger fires (Figure 4). Because of the high similarity between the three datasets, we accept that the datasets provide similar results for large fires; thereby justifying our further comparative analysis.

2.4.2 BA Threshold Results

The dNBR "detects changes in vegetation consumed or killed," (Lentile et. al., 2009) and at smaller area thresholds, results reveal noise due to smaller-scale changes such as clear cuttings (Figure 5, 6). Our findings present relatively similar burned areas between fire products for

comparatively large fires with greater dissimilarity occurring between data products for smaller fires. When we compare the MODIS MCD64A1 burned area product and burned area results derived from Sentinel-2 , we find that both datasets presented similar burned area values for fires 500 acres and larger, while for fires less than 500 acres Sentinel-2 reported significantly higher burned area values (possibly due to MODIS pixel resolution, Figure 7). Because of this discrepancy, we evaluate fires 500 acres and greater on all datasets for the rest of this analysis. Still, when we account for smaller fires, even just fires greater than or equal to 500 acres, we begin to see dramatic increases in the total burned area reported as the spatial resolution of the product increases. For example, figure 8 depicts our comparison of the cumulative burned area for all fires 500 acres and greater between the Sentinel-2, MTBS and MODIS data products. In this figure one can see that for fires 1000 acres and larger (i.e. a threshold of 1000 acres), the MTBS product reports the lowest total burned area (approximately 49,000 acres) while MODIS reports a slightly greater cumulative burned area (approximately 61,000 acres) and the Sentinel-2 dataset reported the greatest burned area (approximately 91,000 acres). When we summarize the burned area totals for all fires 500 acres and greater we find a difference of nearly 57,000 acres between the total burned area reported by MTBS and Sentinel-2 for our study area during the observation month of February 2016 (Table 3).

2.4.3 Spatial distribution Results

The Kernel Smoothed Intensity, which indicates the estimated intensity of the fire occurrence pattern per square meter, was estimated using a Gaussian kernel (Figure 9). The Kernel Smoothed Intensity (KSI) plot for the Sentinel-2 product indicated four major hotspots for fire occurring throughout the primary bounding box of the study region. The MODIS MCD64A1

product showed similar results, save one hotspot in the northern-most portion of the study area. The MTBS KSI plot, on the other hand, indicated a large lack of fire activity throughout the entire central portion of the study region. Hence, the Sentinel-2 and MODIS data products tend to pick up on the same hotspots (or regions with increased fire occurrence) while the MTBS product fails to recognize the same spatial patterns as the products of higher spatial resolution.

2.4.4 Fire Wildland-urban interface analysis results

We found that the WUI comprised a total of 2% of the total study area, with the WUI_x representing 7.2%, urban areas; 4.9%, and the wildland areas equating to 85.2%. The results of our wildland-urban interface analysis indicate that the vast majority (> 96%) of burned area is occurring within our wildland category (Figure 10). This means that we find a relatively larger amount of burned area in the wildlands compared to what would be expected based on area alone. We also find that while the WUI_x category covers more than 7% of the land surface, less than 1.2% of the burned areas can be found in this area. This means that there are relatively fewer fires in the WUI_x category than we would expect by uniform random change. The WUI occupies about 2% of the study area, but the burned area was less than 0.02%, revealing the smaller amount of burned area in WUI. Thus, our results show that we find fewer fires in the WUI and WUI_x areas than would be expected based on the amount of area these classes cover.

2.5 Discussion

All remotely-sensed fire products are imperfect in one way or another and aspects such as the temporal sampling and spatial resolution of the data can cause significant fluctuations or underestimations in burned area outcomes. In addition, while burned areas are easily distinguishable on the ground, the spectral signal of the char can be short-lived, especially in regions dominated by fine fuels where charred vegetation is quickly disseminated via wind (Trigg and Flasse, 2000; Pereira, 2003). Because the spectral signal of char can be fleeting, the acquisition dates for the pre-fire and post-fire imagery can have a significant effect on the burned area that is reported. We started our analyses comparing the MTBS data with other burned area datasets. Our results indicate that for large fires (>1000 acres), datasets report highly similar burned areas regardless of the spatial resolution of the dataset. However, when accounting for smaller fires, even just fires greater than or equal to 500 acres, our results demonstrate that increases in burned area upwards of 57,000 acres. This result supports the findings of Randerson et. al., (2012) which found that accounting for small fires increased global burned area by 35%, with some continental-scale regions such as Equatorial Asia having increases as much as 157%. In addition, Nogueira et. al., (2017) also found that large-scale global burned area products miss between 4% and 15% of the burned area in Brazilian savannas due to missing small fires and note that the omission of small fire patches (<450 ha) in global burned area products is high with omission errors ranging from 0.7 to 0.95.

Oliveira et. al., 2012 noted that fire occurrence information aids in the determination of fire risk by indicating where ignition sources are located and where there are favorable conditions for fire spread. Here we characterized the spatial distribution of fire occurrence by estimating the kernel smoothed intensity of point patterns created by taking the centroid of each

fire over 500 acres from each of the data products. The results of our kernel smoothed intensity functions indicate that the Sentinel-2 and MODIS MCD64A1 products present very similar spatial distributions and intensities of burned areas, while the MTBS presented different results. We believe that this is a result of the fact that the MTBS product only mapped large fires which occurred less frequently than the smaller fires seen on the MODIS and Sentinel-2 products; hence the increased number of fire observations that occurred with the higher resolution products likely yielded more accurate representations of fire intensity. Others have found similar results. For example, Dadashi (2018) found that in the Western United States, the MODIS MCD64A1 product detected 603 more fires than the MTBS product, with 550 of those fires falling below the MTBS threshold of 1000 acres. Vaillant et. al., (2016) also found that the MODIS sensor was able to register more fires than the MTBS dataset for the entire United States. Spatial patterns of fire occurrence are important for risk and natural resource managers (Koutsias et. al., 2004); hence, the capacity of the MTBS product to frequently miss or omit fire events, should be taken into account when proceeding with location or occurrence-based fire projects.

While WUI growth has been linked with an increase in wildfire ignitions (Radeloff et al. 2018), we have demonstrated that the total amount of burned area is relatively small in WUI areas. Our results indicate that within our study region the vast majority of burned area (>96%) is located on wildlands, with minimal burned area detected in the WUI (< .02%) or WUI_x (<1.2%). By determining the proportion of burned area to total area for each of the four land cover categories used (Wildland, Urban, WUI, WUI_x) we found that fewer fires and acres burned than would be expected in the WUI and WUI_x based on the amount of area these classes cover. Hence, for our study area, we find the impacts of wildfires may be greater within the wildlands as opposed to the WUI. Others have found similar ratios of land area. For example, Kramer et.

al. (2018) calculated the area and percentage of intermix, interface, and non- WUI regions within MTBS fire perimeters that contained buildings and found that only 0.4% of the WUI burned between 2000 and 2013. One study in California found that both the population density and the proportion of WUIx land were much stronger correlated ($p< 0.001$) with the number of fires then with the area burned (Syphard et al. 2007). A potential explanation for the small percentage of burned area that we found in the WUI is that while there might be more fires in the WUI, these fires are often small and quickly extinguished (Massada et. al., 2009), in addition to the fact that extensive and uninterrupted wildland fuels typically exist outside of the WUI (Kramer et. al., 2018). In addition, a significant portion of wildland fire suppression and wildland fuel treatments occur in the WUI (Mell et al. 2010). These results appear to be a global trend. For example, despite an increasing global population, the global burned area has reportedly declined by almost 25% between 1998 and 2015 (Andela et al. 2017), with major declines in savannas and grasslands because of human fire constraints.

Still, it has been noted that while the probability of home exposure to wildfire is influenced by the presence of homes in fire-prone areas, it is also influenced by the occurrence of fire and the size and intensity of fire (Calkin et. al., 2014). Hence, as our results indicate that increased fire occurrence is taking place within wildlands or non-WUI regions, it is possible that homes within these wildlands (with a housing density too low to register as WUI) face an even greater risk. Wildfire incidence might be higher among isolated houses even though higher housing density is associated with increased fire risk (Herrero-Corral et. al.,2012). Still, despite the structural risks' fires pose, when looking at the impacts of burned area alone, it is clear that fire management and risk assessment within wildlands should remain a priority.

As of 2010, the WUI comprised 9.5% of the land in the conterminous United States with 33.2% of housing units and 31.9% of the population residing in these WUI areas. Comparatively, in 2010, only 7.6% of the land area in Oklahoma was defined as WUI with 37.3% of the housing units and 36.7% of the population in the state residing within that 7.6% of land indicating that while the percentage of WUI in Oklahoma is slightly less than that of the entire continental U.S., a greater proportion of housing units and people reside within those areas (Radeloff et.al., 2018). According to the National Interagency Fire Center (2019), 745,097 acres burned in the state of Oklahoma in 2018, thereby making Oklahoma the state with the 4th -largest burned area (behind California with 1,823,153 burned acres; Nevada with 1,001,966 burned acres; and Oregon with 897,263 acres burned.) Similarly, in work done by Kramer et. al., (2018), Oklahoma also ranked 4th in states with the highest number of buildings destroyed by wildfire between the years 2000 and 2013. Of those buildings destroyed, 25-50% of them were located within the WUI (here, California also ranked first with 75- 100% of the buildings destroyed by wildfire existing within the WUI)(Kramer et. al., 2018). Hence, although the state of Oklahoma is at high risk for burning and experiencing the destruction of homes due to wildfire compared to the rest of the United States, many (50-75%) of the homes destroyed in the state reside outside of the WUI (dissimilar to states such as California) despite Oklahoma having a slightly higher proportion of housing units and people living within WUI. This information strengthens our conclusion that for the state of Oklahoma, fire management and risk assessments should continue to focus on regions outside of the WUI.

2.6 Conclusion

Overall, despite the Monitoring Trends in Burn Severity program providing highly-detailed, free and user-friendly data, MTBS frequently misses many fires and fails to accurately represent total burned area or the distribution of fire occurrence due to its imposed fire size limitations. On the other hand, the MODIS MCD64A1 product was found to pick up the majority of large fires and more accurately depict fire distribution despite its coarse resolution. We found the higher resolution of the Sentinel-2 based dNBR product significantly increased the total burned area values for our study area indicating that spatial resolution does have a significant impact on burned area. Additionally, our Sentinel-2 product had the capacity to properly depict both larger and mid-range fires while accurately depicting fire distribution, however, the product was still unable to pick up very small fires due to increased noise in the data at small thresholds. Regardless of product, however, the majority of burned area occurred outside of the wildland urban interface and intermix indicating that wildlands and the isolated homes within them may face the greatest risk.

Tables and Figures

Table 1. Examples of currently available remotely-sensed burned area datasets.

Derived product	**Sensor**	**Temporal coverage**	**Spatial resolution**	**Temporal resolution**	**Source**
FireCCILT10	AVHRR-LTDR	1982-2017	0.25 deg	Monthly	Otón & Pettinari, 2019
MTBS	LANDSAT TM/ ETM+/OLI	1984-present	30m*	----	Eidenshink et. al., 2007
PROBA-V	SPOT VGT	2014-present	300 m	10-day composite updated daily	Dierckx et. al., 2014
GFED4	MODIS 500, TRMM/VIRS, ASTR	1995-2016/present	0.25 deg	Monthly / Daily	Giglio et. al., 2013.
MODIS burned area product (MCD45A1, MCD64A1)	MODIS 500m	2000-present	500 m	Monthly / Daily	Giglio et. al., 2016

Table 2. Description of Sentinel-2 Imagery.

Product	Pre-fire Image	Post-fire Image
Tile T15STV		
Entity ID	S2A_MSIL1C_20151204T170702_N0204_R069_T15STV_20151204T170659	S2A_MSIL1C_20160303T170302_N0201_R069_T15STV_20160303T170854
Acquisition Date	12/04/2015	03/03/2016
Tile T15STU		
Entity ID	S2A_MSIL1C_20160103T170712_N0201_R069_T15STU_20160103T170713	S2A_MSIL1C_20160303T170302_N0201_R069_T15STU_20160303T170854
Acquisition Date	01/03/2016	03/03/2016
Platform	Sentinel 2A	Sentinel 2A

Table 3. Results of burned area analysis for all fires greater than or equal to 500 acres within the study area.

Burned Area Analysis Results	
Product	**Total burned area (acres)**
MTBS	48,645
MODIS MCD64A1	69,189
Sentinel-2 dNBR	105,596

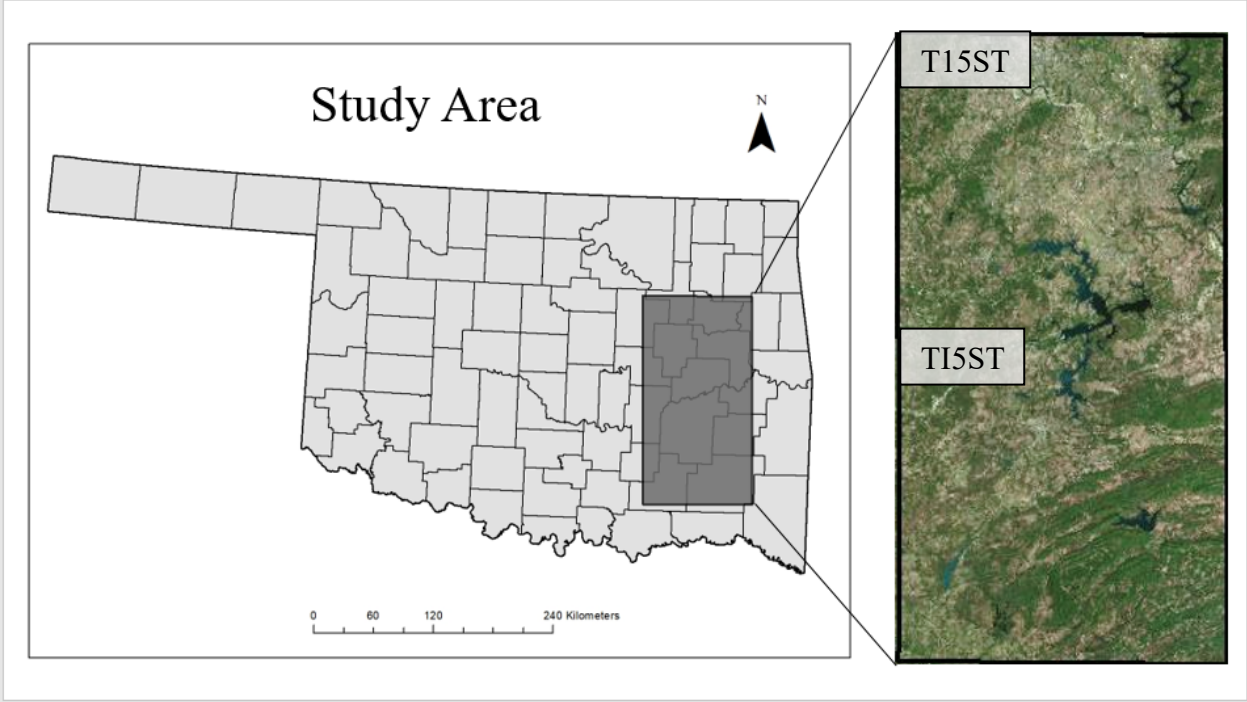

Figure 1. Study area in eastern Oklahoma, USA. The study area is comprised of two adjacent Sentinel-2 tiles, with tile T15STV representing the northern half of the study area and tile T15STU representing the southern half.

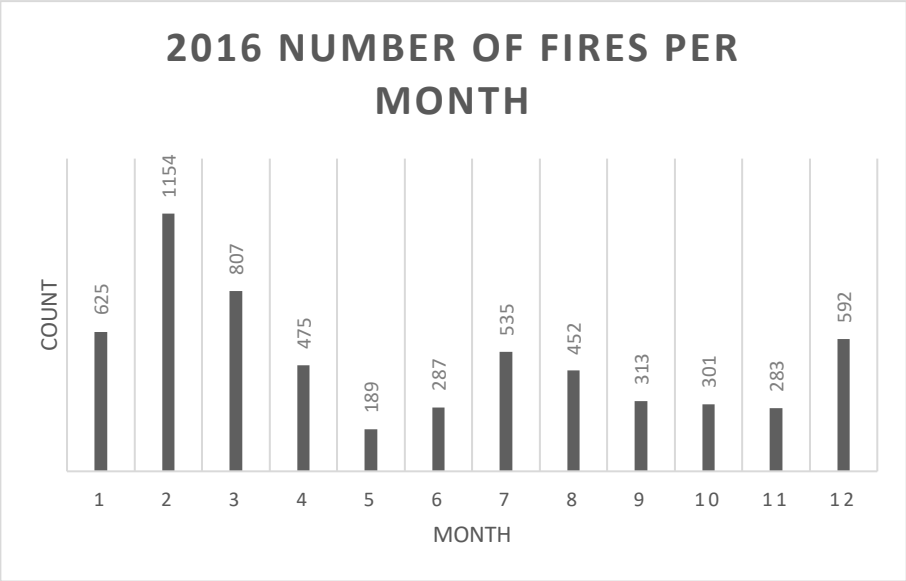

Figure 2. The number of fires occurring per month in Oklahoma in 2016 according to data obtained from the Oklahoma National Fire Incident Reporting System (NFIRS).

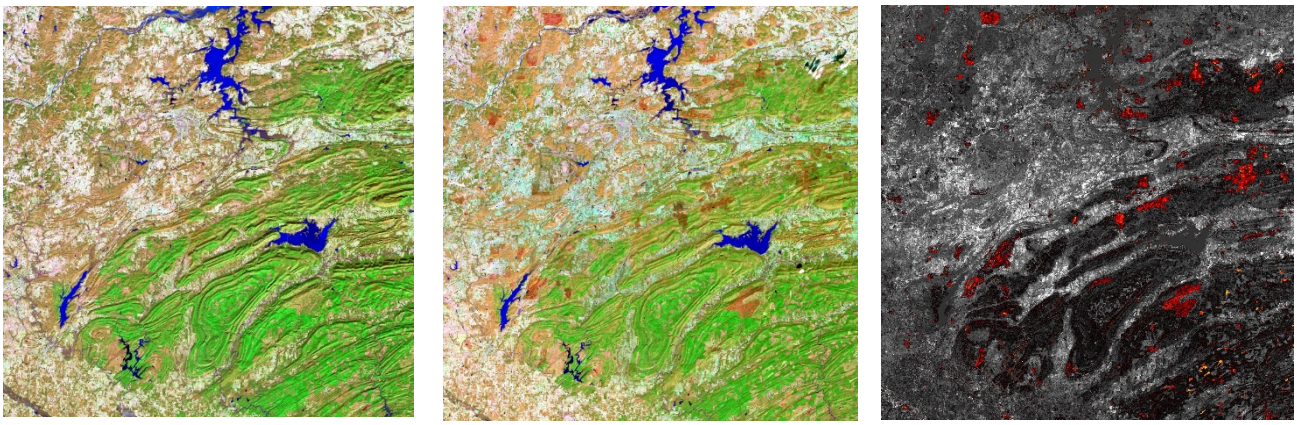

Figure 3. The pre (left) and post-fire (middle) false color images are created from Sentinel-2 T15STU bands 12 (red), 8a (green) and 3 (blue). The burned areas are easily visible on the post-fire image and the dNBR image (right).

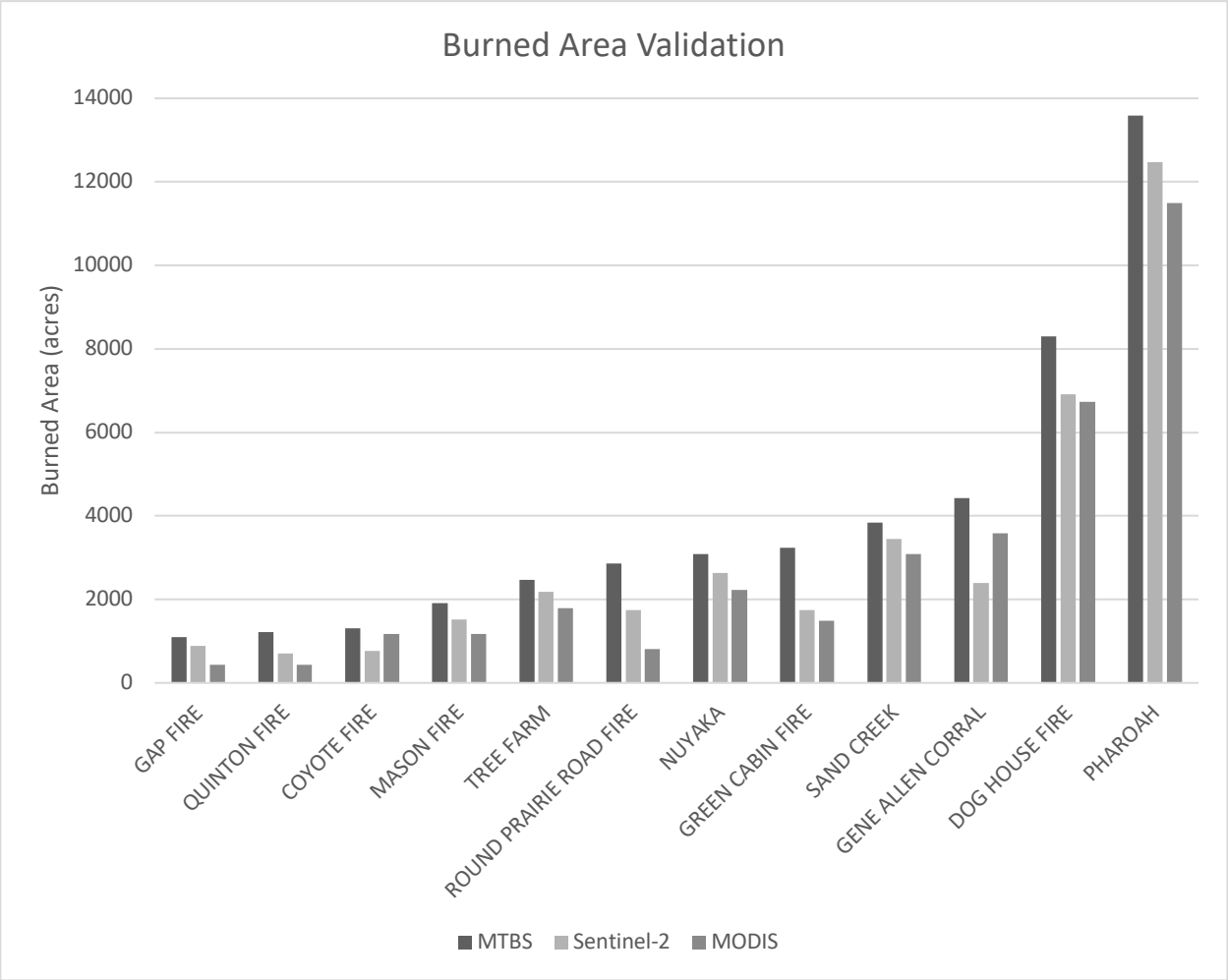

Figure 4. Area burned for the 12 fires observed in the study area by MTBS in February 2016. The fires are listed by name. The Sentinel and MODIS burned area data reveal slight underestimations of the burned areas as compared to the MTBS burned area data. The difference between the datasets appears to be slightly greater for the larger fires.

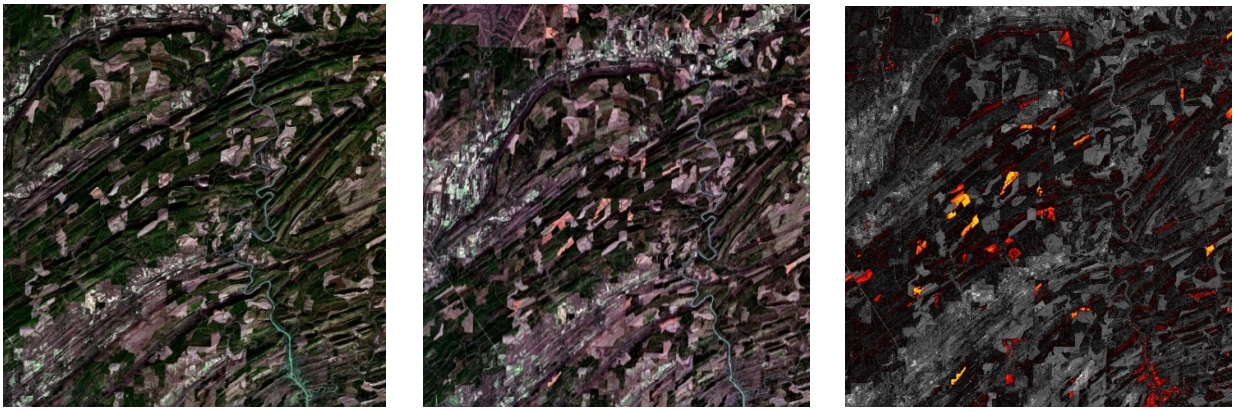

Figure 5. An example of clear-cutting being perceived as fire through dNBR. On the far left, the true color image was captured on 01/03/2016. The image in the center was captured two months later on 03/03/2016. In the center image, one can see evidence of additional clear-cutting that occurred since the image at left was captured. The resulting loss of vegetation due to clear cutting is incorrectly perceived as fire in the dNBR image at right.

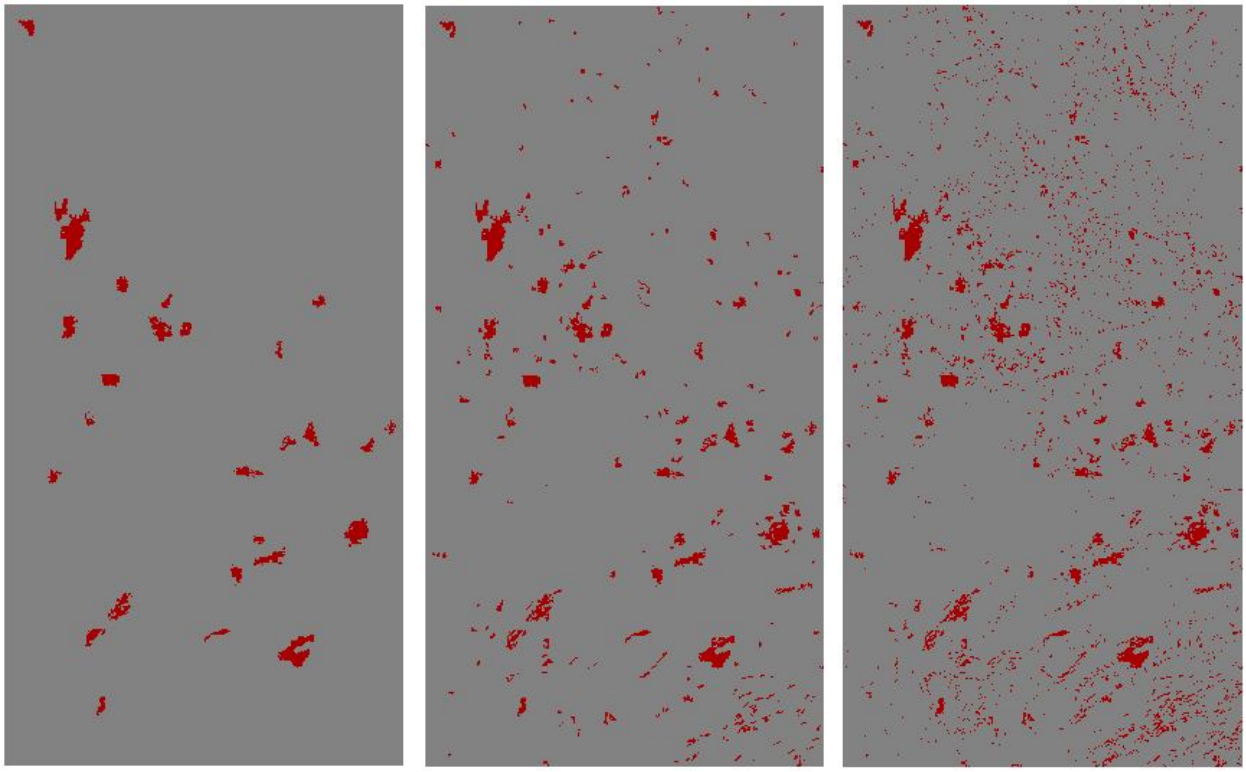

Figure 6. Example of increased noise appearing at smaller thresholds for the Sentinel-2 dataset. The image on the far left depicts all fires over 1000 acres; the image in the center depicts all fires over 100 acres, and the image at right depicts all fires over 10 acres.

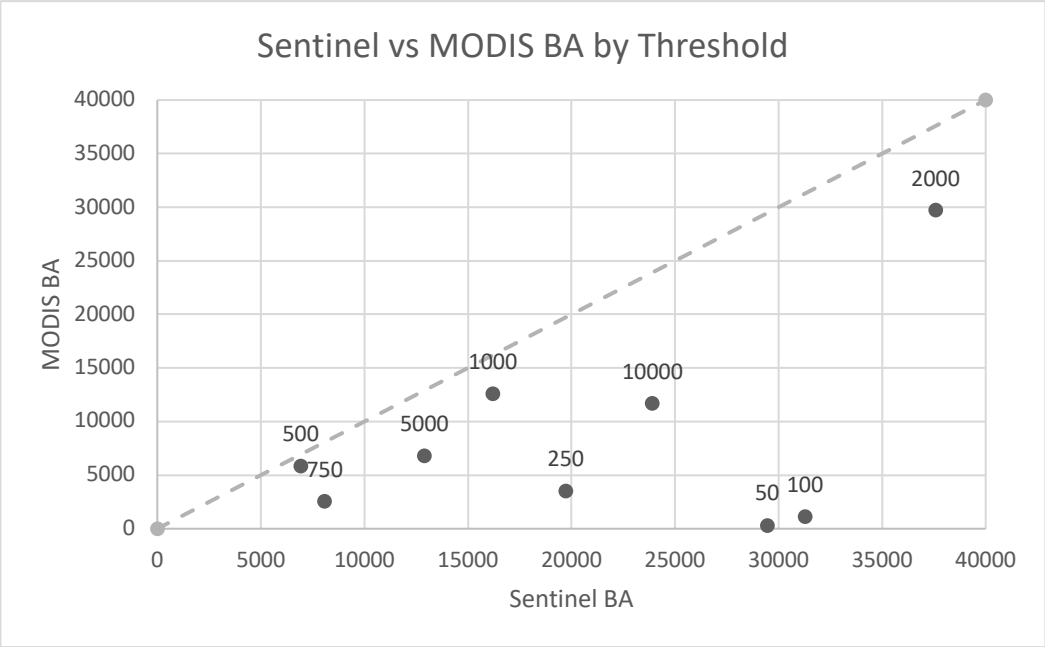

Figure 7. The correlation between burned area and threshold size for the Sentinel-2 and MODIS MCD64A1 datasets. Here, the labels on the points represent threshold size (in acres). Fires less than 500 acres depict significantly greater burned areas for the Sentinel data which could be attributed to the spatial resolution of MODIS (1 pixel is ~ 60 acres) and the capacity of the product to detect smaller fires. There are two fires larger than 10,000 acres, however, MODIS misses one of the fires.

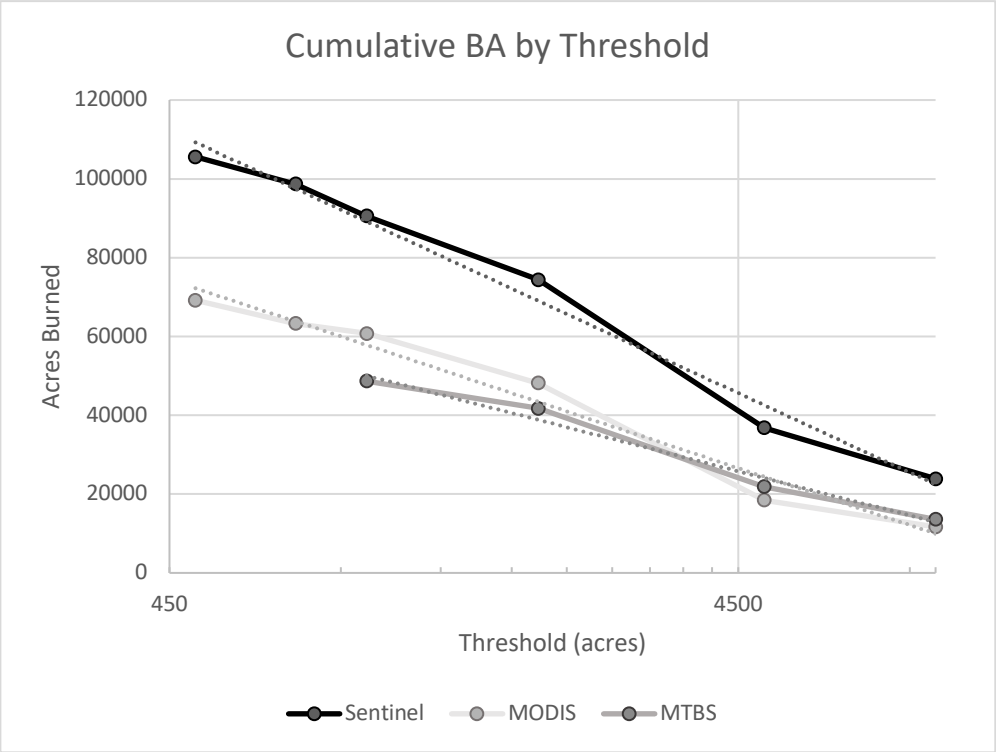

Figure 8. Comparison of the cumulative burned area for all fires 500 acres and greater between the Sentinel-2, MTBS and MODIS data products. Here, the x-axis uses the logarithmic scale and indicates the fire threshold size in acres while the y-axis indicates the total area burned for all fires greater than or equal to the corresponding threshold size. (i.e. For the Sentinel data, all fires 500 acres and greater had a cumulative burned area of approximately 105,000 acres; but for all fires 5000 acres and greater there was a cumulative burned area of approximately 37,000 acres; etc.)

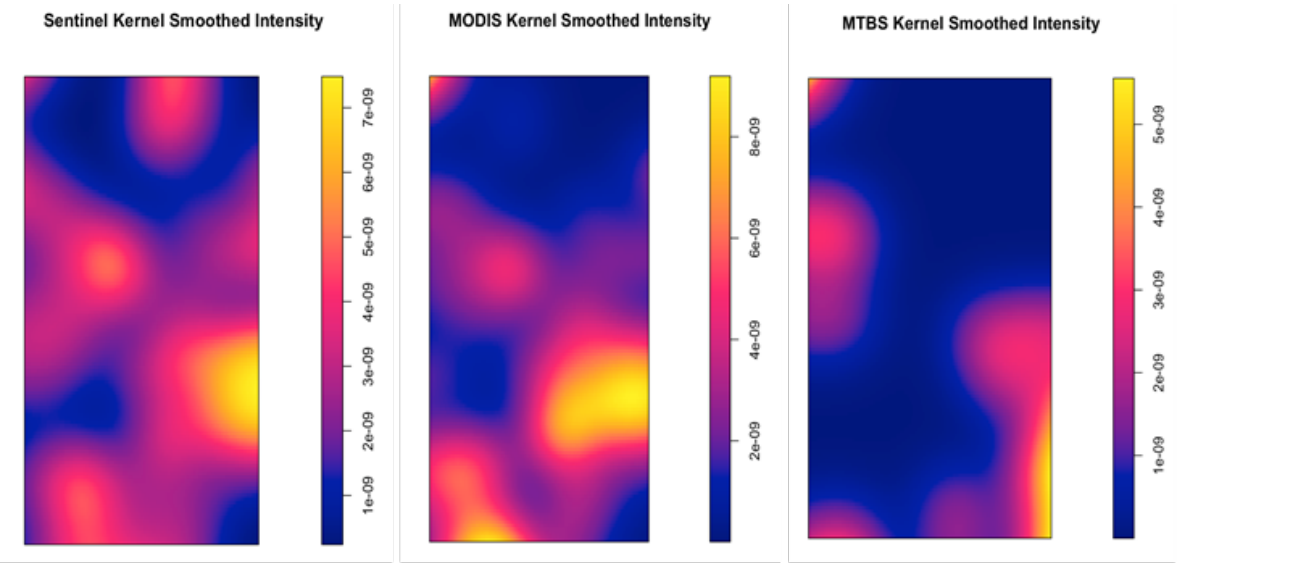

Figure 9. Kernel Smoothed Intensity Plots of fire occurrence for each dataset. Here, the scale indicates the estimated intensity of the fire occurrence pattern per square meter. The Sentinel and MODIS data products tend to pick up on the same hotspots (or regions with increased fire occurrence), save MODIS missing one hotspot in the northern region of the study area. Note that the MTBS product fails to recognize the same spatial patterns.

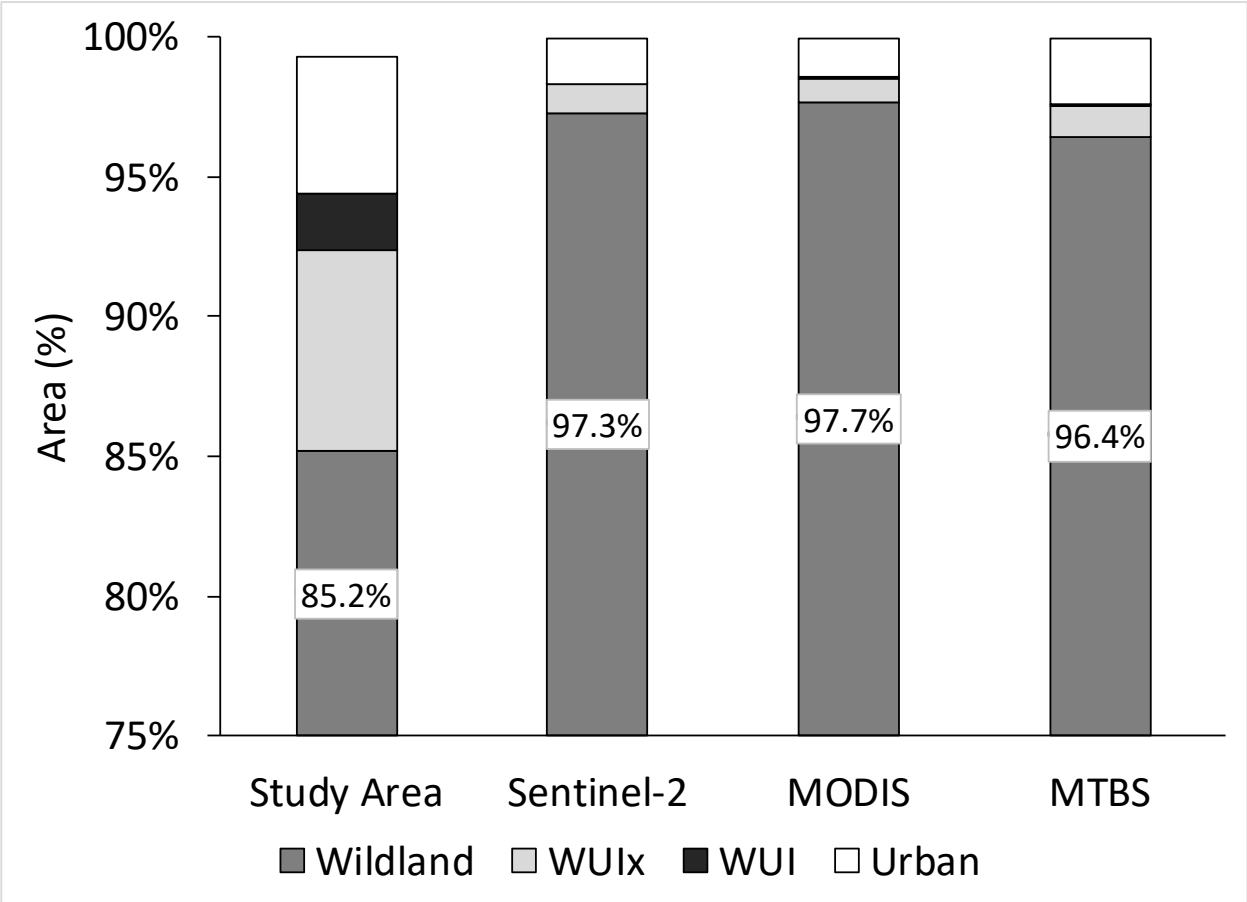

Figure 10. The bar labelled "Study Area" indicates the breakdown of each of our four land cover categories within the study region (by percentage) as indicated by the NLCD data. All other bars indicate the percentage of area that lied within the fire perimeters of the listed dataset by category. Note that all categories *within* fire perimeters are considered to be burned. In our study region, the percentage of area burned is disproportionally higher in wildlands than in any other area. It is possible that we see this trend because the lack of human presence within the wildlands means fires are not reported on or extinguished as quickly as they would be within urban or WUI areas. All three burned area datasets reveal that approximately 97% of all burned areas are found in the wildlands of the study area, despite the fact that just 85% of the study area is classified as wildlands. Additionally, while about 7% of the study area is classified as WUIx, only about 1% of the burned areas are found in the WUIx.

References

Allen, M. S., & Palmer, M. W. (2011). Fire history of a prairie/forest boundary: more than 250 years of frequent fire in a North American tallgrass prairie. *Journal of Vegetation Science*, *22*(3), 436-444.

Allred, B. W., Fuhlendorf, S. D., Engle, D. M., & Elmore, R. D. (2011). Ungulate preference for burned patches reveals strength of fire–grazing interaction. *Ecology and Evolution*, *1*(2), 132-144.

Bar-Massada, A., Radeloff, V. C., & Stewart, S. I. (2014). Biotic and abiotic effects of human settlements in the wildland–urban interface. *Bioscience*, *64*(5), 429-437.

Barrett, D. C. (2015). *Monitoring eastern Oklahoma lake water quality using Landsat* (Doctoral dissertation).

Boyd, C. S., & Bidwell, T. G. (2001). Influence of prescribed fire on lesser prairie-chicken habitat in shinnery oak communities in western Oklahoma. *Wildlife Society Bulletin*, 938-947.

Bright, E. G., Gill, M., Barrientes, A., & Bergey, E. A. (2016). Fire resilience of aquatic crustacean resting stages in playa wetlands, Oklahoma, USA. *Fire Ecology*, *12*(3), 26.

Calkin, D. E., Cohen, J. D., Finney, M. A., & Thompson, M. P. (2014). How risk management can prevent future wildfire disasters in the wildland-urban interface. *Proceedings of the National Academy of Sciences*, *111*(2), 746-751.

Carmona-Moreno, C., Belward, A., Malingreau, J. P., Hartley, A., Garcia-Alegre, M., Antonovskiy, M., ... & Pivovarov, V. (2005). Characterizing interannual variations in global fire calendar using data from Earth observing satellites. *Global Change Biology*, *11*(9), 1537-1555.

Clark, S. L., Hallgren, S. W., Engle, D. M., & Stahle, D. W. (2007). The historic fire regime on the edge of the prairie: a case study from the Cross Timbers of Oklahoma. In *Proceedings of the Tall Timbers Fire Ecology Conference* (Vol. 23, pp. 40-49).

Dadashi, S. (2018). What Is a Fire? Identifying Individual Fire Events Using the MODIS Burned Area Product

Dennison, P. E., Brewer, S. C., Arnold, J. D., & Moritz, M. A. (2014). Large wildfire trends in the western United States, 1984–2011. *Geophysical Research Letters*, *41*(8), 2928-2933.

Dierckx, W., Sterckx, S., Benhadj, I., Livens, S., Duhoux, G., Van Achteren, T., ... & Saint, G. (2014). PROBA-V mission for global vegetation monitoring: standard products and image quality. *International Journal of Remote Sensing*, *35*(7), 2589-2614.

Diggle, P. (1985). A Kernel Method for Smoothing Point Process Da-ta. Journal of the Royal Statistical Society. Series C (Applied Statistics), 34(2), 138-147. doi:10.2307/2347366

Eidenshink, J., Schwind, B., Brewer, K., Zhu, Z. L., Quayle, B., & Howard, S. (2007). A project for monitoring trends in burn severity. *Fire ecology*, *3*(1), 3-21.

Fann, N., Alman, B., Broome, R. A., Morgan, G. G., Johnston, F. H., Pouliot, G., & Rappold, A. G. (2018). The health impacts and economic value of wildland fire episodes in the US: 2008–2012. *Science of the total environment*, *610*, 802-809.

Flannigan, M. D., Krawchuk, M. A., de Groot, W. J., Wotton, B. M., & Gowman, L. M. (2009). Implications of changing climate for global wildland fire. *International journal of wildland fire*, *18*(5), 483-507.

Fornacca, D., Ren, G., & Xiao, W. (2018). Evaluating the Best Spectral Indices for the Detection of Burn Scars at Several Post-Fire Dates in a Mountainous Region of Northwest Yunnan, China. *Remote Sensing*, *10*(8), 1196.

Giglio, L., Randerson, J. T., & van der Werf, G. R. (2013). Analysis of daily, monthly, and annual burned area using the fourth-generation global fire emissions database (GFED4). *Journal of Geophysical Research: Biogeosciences*, *118*(1), 317-328.

Giglio, L., Boschetti, L., Roy, D., Hoffmann, A. A., & Humber, M. (2016). Collection 6 MODIS Burned Area Product User's Guide Version 1.0. *NASA EOSDIS Land Processes DAAC: Sioux Falls, SD, USA*.

Gitas, I. Z., Mitri, G. H., & Ventura, G. (2004). Object-based image classification for burned area mapping of Creus Cape, Spain, using NOAA-AVHRR imagery. *Remote Sensing of Environment*, *92*(3), 409-413.

Grégoire, J. M., Tansey, K., & Silva, J. M. N. (2003). The GBA2000 initiative: developing a global burnt area database from SPOT-VEGETATION imagery. *International Journal of Remote Sensing*, *24*(6), 1369-1376.

Greenberg, J. D., & Bradley, G. A. (1997). Analyzing the urban-wildland interface with GIS: Two case studies. *Journal of Forestry*, *95*(10), 18-22.

Guindos-Rojas, F., Arbelo, M., García-Lázaro, J., Moreno-Ruiz, J., & Hernández-Leal, P. (2018). Evaluation of a Bayesian Algorithm to Detect Burned Areas in the Canary Islands' Dry Woodlands and Forests Ecoregion Using MODIS Data. *Remote Sensing*, *10*(5), 789.

Hall, J. V., Loboda, T. V., Giglio, L., & McCarty, G. W. (2016). A MODIS-based burned area assessment for Russian croplands: Mapping requirements and challenges. *Remote Sensing of Environment*, *184*, 506-521.

Hammer, R. B., Stewart, S. I., & Radeloff, V. C. (2009). Demographic trends, the wildland–urban interface, and wildfire management. *Society and Natural Resources*, *22*(8), 777-782.

Herrero-Corral, G., Jappiot, M., Bouillon, C., & Long-Fournel, M. (2012). Application of a geographical assessment method for the characterization of wildland–urban interfaces in the context of wildfire prevention: A case study in western Madrid. *Applied Geography*, *35*(1-2), 60-70.

Hussain, M., Chen, D., Cheng, A., Wei, H., & Stanley, D. (2013). Change detection from remotely sensed images: From pixel-based to object-based approaches. *ISPRS Journal of photogrammetry and remote sensing*, *80*, 91-106.

Jean-Francois Pekel, Andrew Cottam, Noel Gorelick, Alan S. Belward, High-resolution mapping of global surface water and its long-term changes. Nature 540, 418-422 (2016). (doi:10.1038/nature20584)

Kennedy, R. E., Townsend, P. A., Gross, J. E., Cohen, W. B., Bolstad, P., Wang, Y. Q., & Adams, P. (2009). Remote sensing change detection tools for natural resource managers: Understanding concepts and tradeoffs in the design of landscape monitoring projects. *Remote sensing of environment*, *113*(7), 1382-1396.

Koutsias, N., Kalabokidis, K. D., & Allgöwer, B. (2004). Fire occurrence patterns at landscape level: beyond positional accuracy of ignition points with kernel density estimation methods. *Natural Resource Modeling*, *17*(4), 359-375.

Koutsias, N., Karteris, M., & Chuvico, E. (2000). The use of intensity-hue-saturation transformation of Landsat-5 Thematic Mapper data for burned land mapping. *Photogrammetric Engineering and Remote Sensing*, *66*(7), 829-840.

Kramer, H. A., Mockrin, M. H., Alexandre, P. M., Stewart, S. I., & Radeloff, V. C. (2018). Where wildfires destroy buildings in the US relative to the wildland–urban interface and national fire outreach programs. *International journal of wildland fire*, *27*(5), 329-341.

Lentile, L. B., Holden, Z. A., Smith, A. M., Falkowski, M. J., Hudak, A. T., Morgan, P., ... & Benson, N. C. (2006). Remote sensing techniques to assess active fire characteristics and post-fire effects. *International Journal of Wildland Fire*, *15*(3), 319-345.

Lentile, L. B., Smith, A. M., Hudak, A. T., Morgan, P., Bobbitt, M. J., Lewis, S. A., & Robichaud, P. R. (2009). Remote sensing for prediction of 1-year post-fire ecosystem condition. *International Journal of Wildland Fire*, *18*(5), 594-608.

Libonati, R., DaCamara, C., Setzer, A., Morelli, F., & Melchiori, A. (2015). An algorithm for burned area detection in the Brazilian Cerrado using 4 μm MODIS imagery. *Remote Sensing*, *7*(11), 15782-15803.

Lutes, D. C., Keane, R. E., Caratti, J. F., Key, C. H., Benson, N. C., Sutherland, S., & Gangi, L. J. (2006). FIREMON: Fire effects monitoring and inventory system. *Gen. Tech. Rep. RMRS-GTR-164. Fort Collins, CO: US Department of Agriculture, Forest Service, Rocky Mountain Research Station. 1 CD.*, *164*.

Massada, A. B., Radeloff, V. C., Stewart, S. I., & Hawbaker, T. J. (2009). Wildfire risk in the wildland–urban interface: a simulation study in northwestern Wisconsin. *Forest Ecology and Management*, *258*(9), 1990-1999.

Mohler, R. L., & Goodin, D. G. (2012). Mapping burned areas in the Flint Hills of Kansas and Oklahoma, 2000—2010. *Great Plains Research*, 15-25.

National Interagency Fire Center. (2019). National Report of Wildland Fires and Acres Burned by State. Retrieved from: https://www.predictiveservices.nifc.gov/intelligence/2018_statssumm/fires_acres18.pdf

Nogueira, J., Ruffault, J., Chuvieco, E., & Mouillot, F. (2017). Can we go beyond burned area in the assessment of global remote sensing products with fire patch metrics?. *Remote Sensing*, *9*(1), 7.

Oliveira, S., Oehler, F., San-Miguel-Ayanz, J., Camia, A., & Pereira, J. M. (2012). Modeling spatial patterns of fire occurrence in Mediterranean Europe using Multiple Regression and Random Forest. *Forest Ecology and Management*, *275*, 117-129.

Otón, G., & Pettinari, M. L. ESA Climate Change Initiative–Fire_cci D3. 3.4 Product User Guide–AVHRR-Long Term Data Record (PUG-LTDR).

Padilla, M., Stehman, S. V., Ramo, R., Corti, D., Hantson, S., Oliva, P., ... & Pereira, J. M. (2015). Comparing the accuracies of remote sensing global burned area products using stratified random sampling and estimation. *Remote sensing of environment*, *160*, 114-121.

Pereira, J. M. (2003). Remote sensing of burned areas in tropical savannas. *International Journal of Wildland Fire*, *12*(4), 259-270.

Plummer, S., Arino, O., Simon, M., & Steffen, W. (2006). Establishing a earth observation product service for the terrestrial carbon community: The GLOBCARBON initiative. *Mitigation and adaptation strategies for global change*, *11*(1), 97-111.

Randerson, J. T., Chen, Y., Van Der Werf, G. R., Rogers, B. M., & Morton, D. C. (2012). Global burned area and biomass burning emissions from small fires. *Journal of Geophysical Research: Biogeosciences*, *117*(G4).

Simon, M., Plummer, S., Fierens, F., Hoelzemann, J. J., & Arino, O. (2004). Burnt area detection at global scale using ATSR-2: The GLOBSCAR products and their qualification. *Journal of Geophysical Research: Atmospheres*, *109*(D14).

Sparks, A. M., Boschetti, L., Smith, A. M., Tinkham, W. T., Lannom, K. O., & Newingham, B. A. (2015). An accuracy assessment of the MTBS burned area product for shrub–steppe fires in the northern Great Basin, United States. *International Journal of Wildland Fire*, *24*(1), 70-78.

Stambaugh, M. C., Guyette, R. P., & Marschall, J. (2013). Fire history in the Cherokee nation of Oklahoma. *Human Ecology*, *41*(5), 749-758.

Stavros, E. N., McKenzie, D., & Larkin, N. (2014). The climate–wildfire–air quality system: interactions and feedbacks across spatial and temporal scales. *Wiley Interdisciplinary Reviews: Climate Change*, *5*(6), 719-733.

Tansey, K., Grégoire, J. M., Pereira, J. M., Defourny, P., Leigh, R., Barros, A., ... & Bontemps, S. (2007). A global, multi-year (2000-2007), validated burnt area product (L3JRC) derived from daily SPOT VEGETATION data: *towards an operational use of remote sensing in forest fire management*, 154.

Trigg, S., & Flasse, S. (2000). Characterizing the spectral-temporal response of burned savannah using in situ spectroradiometry and infrared thermometry. *International Journal of Remote Sensing*, *21*(16), 3161-3168.

U.S. Census Bureau (2010). *Oklahoma Quick Facts*. Retrieved from https://www.census.gov/quickfacts/fact/table/OK/PST045218

USDA National Agricultural Statistics Service Cropland Data Layer. (2016). Published crop-specific data layer [Online]. Available at https://nassgeodata.gmu.edu/CropScape/ USDA-NASS, Washington, DC.

Vaillant, N. M., Kolden, C. A., & Smith, A. M. (2016). Assessing landscape vulnerability to wildfire in the USA. *Current Forestry Reports*, *2*(3), 201-213.

Veraverbeke, S., Lhermitte, S., Verstraeten, W. W., & Goossens, R. (2010). The temporal dimension of differenced Normalized Burn Ratio (dNBR) fire/burn severity studies: The case of the large 2007 Peloponnese wildfires in Greece. *Remote Sensing of Environment*, *114*(11), 2548-2563.

Yang, J., He, H. S., Shifley, S. R., & Gustafson, E. J. (2007). Spatial patterns of modern period human-caused fire occurrence in the Missouri Ozark Highlands. Forest science, 53(1), 1-15

Yang, L., Jin, S., Danielson, P., Homer, C., Gass, L., Case, A., Costello, C., Dewitz, J., Fry, J., Funk, M., Grannemann, B., Rigge, M. and G. Xian. (2018). A New Generation of the United States National Land Cover Database: Requirements, Research Priorities, Design, and Implementation Strategies, p. 108–123.

Zhu, C., Kobayashi, H., Kanaya, Y., & Saito, M. (2017). Size-dependent validation of MODIS MCD64A1 burned area over six vegetation types in boreal Eurasia: Large underestimation in croplands. *Scientific reports*, *7*(1), 4181.